Structural Engineering and Mechanics, *Vol. 55, No. 5 (2015) 1037-1053*
DOI: http://dx.doi.org/10.12989/sem.2015.55.5.1037

Experimental and numerical analysis of RC structure with two leaf cavity wall subjected to shake table

Onur Onat*[1], Paulo B. Lourenço[2a] and Ali Koçak[3b]

[1]*Department of Civil Engineering, Tunceli University, Tunceli, Turkey*
[2]*Department of Civil Engineering, Minho University, Guimaraes, Portugal*
[3]*Department of Civil Engineering, Yıldız Technical University, İstanbul, Turkey*

(Received April 15, 2015, Revised July 20, 2015, Accepted August 4, 2015)

Abstract. This paper presents finite element (FE) based pushover analysis of a reinforced concrete structure with a two-leaf cavity wall (TLCW) to estimate the performance level of this structure. In addition to this, an unreinforced masonry (URM) model was selected for comparison. Simulations and analyses of these structures were performed using the DIANA FE program. The mentioned structures were selected as two storeys and two bays. The dimensions of the structures were scaled 1:1.5 according to the Cauchy Froude similitude law. A shake table experiment was implemented on the reinforced concrete structure with the two-leaf cavity wall (TLCW) at the National Civil Engineering Laboratory (LNEC) in Lisbon, Portugal. The model that simulates URM was not experimentally studied. This structure was modelled in the same manner as the TLCW. The purpose of this virtual model is to compare the respective performances. Two nonlinear analyses were performed and compared with the experimental test results. These analyses were carried out in two phases. The research addresses first the analysis of a structure with only reinforced concrete elements, and secondly the analysis of the same structure with reinforced concrete elements and infill walls. Both researches consider static loading and pushover analysis. The experimental pushover curve was plotted by the envelope of the experimental curve obtained on the basis of the shake table records. Crack patterns, failure modes and performance curves were plotted for both models. Finally, results were evaluated on the basis of the current regulation ASCE/SEI 41-06.

Keywords: reinforced concrete; shake table; finite element method; infill wall; pushover

1. Introduction

Earthquakes have been a severe and hazardous challenge for most of the countries on the world from ancient times to the present. Turkey, for example, has active faults such as the East Anatolian Fault (EAF) and North Anatolian Fault (NAF), and fatalities from earthquakes along these faults have been studied by many authors. In particular, the NAF caused the loss of thousands of lives and huge economic losses in the Marmara earthquake of 1999, with a magnitude of 7.4 (Bruneau

*Corresponding author, Researcher, E-mail: onat.onur@hotmail.com, onuronat@tunceli.edu.tr
[a]PhD, E-mail: pbl@civil.uminho.pt
[b]PhD, E-mail: akocak@yildiz.edu.tr

http://www.techno-press.org/?journal=sem&subpage=8 ISSN: 1225-4568 (Print), 1598-6217 (Online)

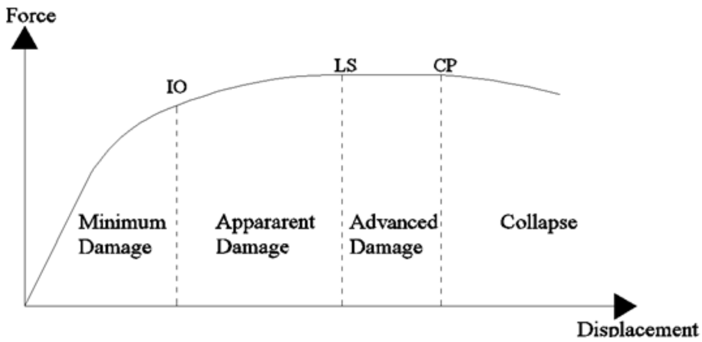

Fig. 1 Performance curve of a typical structure (TEC 2007)

2002). Doğangün (2004) studied the performance of reinforced concrete structures destroyed by the Bingöl earthquake triggered by the EAF and NAF, where the highest measured PGA was 5.45 m/s^2. In 2004, Ağrı Doğubeyazıt was struck by another earthquake close to the starting point of the EAF and NAF. One thousand buildings were affected by this earthquake and 100 houses were severely damaged (Bayraktar *et al*. 2007). Sayın *et al*. (2013) discussed the failures of adobe and masonry buildings in the Maden earthquake of June 2011.They emphasized that even a 5.3 magnitude earthquake can result in unexpected fatalities and economic loss. Another two recent earthquakes in Turkey were the 2011 Simav and 2011 Van earthquakes. The magnitude of the Simav earthquake was lower than that of the Van earthquake at 5.8 (Yön *et al*. 2013). Furthermore, the heaviest fatalities were witnessed in Van, where 607 people were killed, 1301 were injured and 2307 multi-storey buildings collapsed (Kızılkanat *et al*. 2011, Sayın *et al*. 2014). Finally, Tapan *et al*. addressed the seismic and ground motion characteristics of the 2011 Van earthquake and then presented the seismic performance of the structures affected, which were poor, especially school and hospital buildings (Tapan *et al*. 2013).

Turkey and the rest of the world have experienced failure of structures under severe ground motions as presented above. This is one of the big challenges for the construction industry, which is trying to develop better solutions for reinforced concrete structures, especially to make infill walls able to resist strong ground motion. This is important not only to save lives but also to limit economic loss, for both rural and urban territories. This paper contributes to this purpose by discussing the performance and failure modes of a two-leaf cavity wall reinforced concrete structure exposed to an artificial earthquake load. To assess the performance of the TLCW model in this study, an URM model was used as reference. Because the contribution of the infill wall to the structural system provides additional capacity to lateral loads, the URM model was used to compare the performance level of TLCW by contrast with a bare reinforced concrete frame.

2. Brief review of pushover analysis

The most commonly used technique today to assess the performance of a structure is pushover analysis, which has led to the so-called “Performance Based Design”. For nearly four decades, nonlinear static analysis has been used by engineers to estimate the performance of complex new structures and existing structures. In seismic engineering, pushover (nonlinear) analysis allows us to predict the demand requirements of a structure. A credible pushover analysis requires that the structural model should be realistic and the analysis procedure has to be reliable. Structures have different performance characteristics. These are displacement capacity, stiffness and strength. One of the most useful performance characteristics is the displacement capacity. Displacement of the structures can be categorized into three limits, namely serviceability, damage control and collapse prevention. In addition to displacement capacity, which is more effective than others, stiffness is also another important characteristic. However, it is difficult to evaluate stiffness during changing loading conditions. The criteria have to be clear and to reflect the situation of the structure, and this is possible using force-displacement diagrams (Ghobarah 2001). For example, the Turkish Seismic Code (TEC) defines three performance levels using this diagram, as shown in Fig. 1 (TEC 2007).

Fajfar (1999) discussed the use of the capacity spectrum method to compare the capacity of a structure with the demands of the ground motion of an earthquake, proposing the so-called N2 method. Salonikios *et al*. (2003) evaluated existing masonry structures on the basis of FEMA 273, by performing nonlinear analysis. Fajfar (1999) and Salonikios (2003) also proposed stress-strain material laws to see more realistic behaviour of structures and they emphasized that the modelling approach and the material assumptions play a very important role in the structural response obtained. The N2 method has been extended by Dolsek and Fajfar (2005) by applying it to two in-filled reinforced concrete structures and discussing the inelastic demand spectra. They concluded that this type of analysis provides an understanding of the performance of this type of structure. Barros and Almeida (2005) performed pushover analysis for mass asymmetric irregular building frames using three different structural models. It was concluded that the performance of ordinary pushover force depends on the shape of the first vibration mode and that higher vibration modes are important. Yön and Calayır (2014) investigated the effects of confinement and the class of concrete on the nonlinear behaviour of reinforced concrete buildings by pushover analysis. The effect of confinement was to increase the building capacity and decrease the rotations.

The main purpose of plotting pushover curves is to evaluate the lateral bearing capacity of a structure, usually determined by the maximum displacement of the roof level versus base shear (Reinhorn 1997). It is assumed that the level of damage in the curve represents the actual damage to the building at a given target displacement (Moghadam 2000). The prevision of the correct damage mechanism is one another challenge for structural system. Tso and Moghadan (1996), for example, addressed this aspect for multi-storey and eccentric structures. According to these authors, during failure the first mode shape has more influence than the other mode shapes. Kilar and Fajfar (1997) developed a method for nonlinear static analysis of asymmetric buildings, applying a constant incremental lateral load and assuming that the structure is a planar macro element. Here, base shear and roof displacement were taken into consideration. Krawinkler and Seneviranta (1998) addressed the difficulties and benefits of using nonlinear static analysis with a constant incremental ratio. Chopra and Goel (2001) developed a new pushover analysis method that included higher modes of the structure. The basic principle of this method is to adopt the seismic demand of the structure composed of each storey’s inertial moment. Based on these different studies, different performance levels can be established with reasonable reliability for standard structures to estimate their damage in terms of ASCE/SEI 41-06 (2007).

3. Experimental results

A two-leaf cavity infill wall is composed of two leaves between which there is a 2 cm gap. The

(a) Exterior leaf

(b) Complete double leaf

Fig. 2 Two leaf cavity infill wall (Pereira 2013 and Leite 2014)

Fig. 3 Reinforced concrete structure with two leaf cavity infill wall before test (Leite 2014)

exterior leaf is 9 cm and the interior leaf is 7 cm. The total thickness of the wall is 18 cm. This thickness and the whole tested structure were 1.5 times reduced in scale on the basis of Cauchy and Froude's similitude law. The double-leaf infill wall can be seen in Fig. 2.

Before the shake table test, material characterization was first implemented on the concrete and double-leaf infill wall. Then the structure was produced and plastered. Additional masses were attached onto the structure to comply with an unreduced scale structure. The final view of the structure before the shake table test can be seen in Fig. 3.

Table 1 Brief presentation of experiment

Loading	Return Period (Years)	PGA (g)	
		Transversal	Longitudinal
Loading-1	225	0.136	0.176
Loading-2	475	0.217	0.298
Loading-3	2475	0.739	1.05
Loading-4	1.5x2475	0.983	1.07

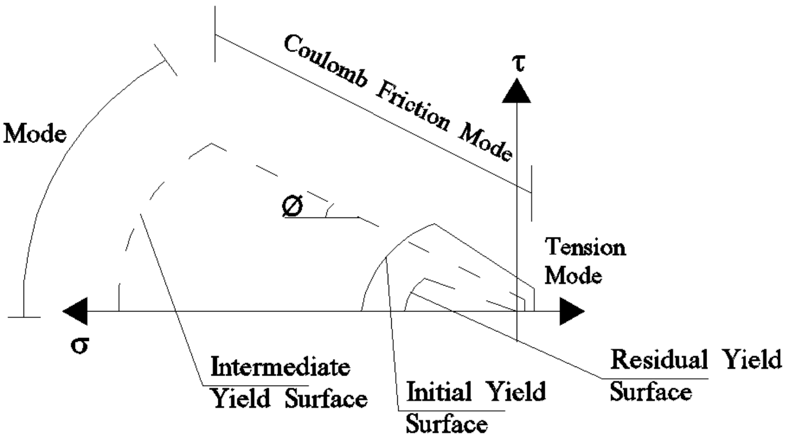

Fig. 4 Coulomb friction model combined with tension cut-off and elliptical compression (Lourenço and Rots 1997)

Shake table tests were carried out on the structure in four loading steps. The loadings are classified according to the return periods of earthquake loading. The return periods and PGA values can be seen in Table 1.

4. Adopted material models

Before structural analysis, realistic material models were defined. In the numeric model, three types of material models were used for concrete, interface and infill. Nonlinear properties were selected based on the crack propagation of each member during the shake table experiments. Total Strain Fixed Crack (CEB-FIB 2012) was used for the reinforced concrete members. The basic properties of the material were calculated using Eurocode-2 (2004) and CEB-FIP 2010 (2012). For the interface between the frame and the masonry infill, the Combined Cracking-Shear-Crush material model was used to simulate tensile crack opening, frictional slip and crushing (Lourenço and Rots 1997). The basic nonlinear properties of the interface material were calculated according to the recommendations of Lourenço (2009). The Total Strain Rotating Crack model was used for the masonry infill (CEB-FIB 2012). It should be stressed that while the Fixed Crack Model simulates well the behaviour of reinforced concrete structures, this material model can overestimate the stiffness response and shear capacity for unreinforced structures. More complex material models are available for masonry, such as the orthotropic model developed by Lourenço *et al*. (1998), but they require a large amount of data, which is not available in many cases. In the present case, as the interface plays an important role, the model adopted for the masonry infill was kept reasonably simple, as isotropic (before cracking).

This material model adopted for concrete and masonry describes the compression and tensile behaviour of material with an adequate stress-strain relationship. This total strain material model was developed along the lines of the Modified Compression Field Theory (Vecchio and Collins 1986), following a smeared approach for the fracture energy (Selby and Vecchio 1993). The fundamental difference between the fixed and rotating concepts is the direction of principal stresses after the onset of cracking. Propagation of cracks is fixed to local coordinates in the first case. However, the propagation of cracks rotates according to the principal stress axes in the second case. The interface model was formulated by Lourenço and Rots (1997) as stated before for plane stress and then implemented by Van Zijl (2000) in 3D. This interface model is based on multi-surface plasticity, including a Coulomb friction model integrated with a tension cut-off and an elliptical compression cap to relate the interface traction σ to the interface shear τ, as shown in Fig. 4. Inelastic behaviour occurs in all failure modes and is preceded by hardening in the case of the cap mode (Lourenço and Rots 1997).

5. Results of the simulation

Nonlinear static analysis was carried out for two structures composed of different masonry infill. First, the reinforced concrete structure with two-leaf cavity wall (TLCW) is considered, because experimental results are available only for this model. After validation of the numerical simulation approach, an unreinforced single-leaf wall is considered (URM). The objective is to simulate traditional structures in many countries, including Turkey, where cavity walls are not common. The structure with the two-leaf cavity masonry wall has an experimental envelope curve obtained by the shake table experiment. The structure with the single-leaf masonry wall was modelled with the same condition and the same parameters as the two-leaf cavity wall. The main purpose of this comparison is to see the contribution of the different solutions to lateral loads. In addition to elastic properties, the nonlinear properties of the structural models are presented next. Phase analysis was used in the analysis to simulate the real condition during construction, as the frames are usually built before the walls and vertical loading is expected to be in the columns beams and slabs, not in the masonry infill. Thus, the reinforced concrete structure was loaded with the self-weight at the first phase, the majority of the weight being due to the slabs, columns and beams. In the second phase, the infill walls were added to the model and loaded again with their self-weight. After that, nonlinear pushover analysis was started by applying a horizontal load proportional to the mass that replicates the inertial forces. This analysis was performed using the Regular Newton-Raphson method with a convergence criterion based on an internal energy tolerance of 10^{-3}.See Fig. 5 for a general flowchart of the usual solution procedure in nonlinear mechanics. The arc-length control method was used, as an indirect displacement control method. The force ratio used to control the response was obtained by Eq. (1) at each iteration step.

$$\alpha_{x,z} = \frac{\sum Horizontal\ Base\ Shear}{Selfweight} \tag{1}$$

The linear and nonlinear parameters are presented in Tables 2 and 3. These properties have been obtained from the experimental study by Pereira and Leite (Pereira 2013, Leite 2014) and are as indicated above. It is noted that interface properties are the most relevant for the analysis and

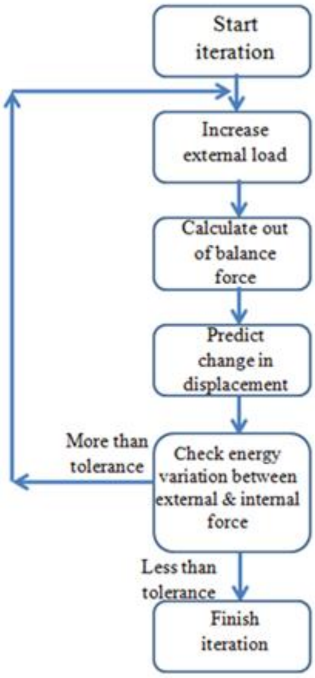

Fig. 5 Flow chart of iteration steps during the nonlinear static analysis

Table 2 Material properties of concrete and infill belong to numeric models

Type of material	Elastic Modulus (MPa)	Compressive Strength, f_c (MPa)	Compressive fracture energy, G_c (N/mm)	Tensile strength, f_t (MPa)	Mode-I fracture energy, G_f^I (N/mm)
Concrete	30400	29.5	47.2	2.32	0.051
Infill	1800	1.26	2.0	0.20	0.013

Table 3 Material properties of interface for numeric models

K_n (N/mm^3)	K_s (N/mm^3)	Tensile Strength, f_t (MPa)	Mode-I Fracture Energy, G_f^I (N/mm)	Mode-II Fracture Energy, G_f^{II} (N/mm)	Friction Coefficients		
					c (cohesion)	$\emptyset$ (friction angle)	Ψ (dilatancy angle)
175	75	0.30	0.012	0.030	0.6	0.75	0.01

the tensile strength and cohesion were adjusted to replicate the experimental capacity curve, and compressive failure was not included in the interface. All other inelastic parameters for the interface were calculated by cited references (Zijl 2000, CUR 1997, Lourenço 1996).

On the basis of the experimental ground motions, envelope curves were plotted along both the transversal and longitudinal directions. Loading of pushover analysis was carried out using DIANA 9.4.4 (TNO 2012) software and the results were plotted in Fig. 8 and Fig. 9, for the transversal and longitudinal directions, respectively. These analyses were performed with both fine mesh and coarse mesh, a view of which can be seen in Fig. 6.

While modelling, the 3-node curved beam element used for the reinforced concrete frame was

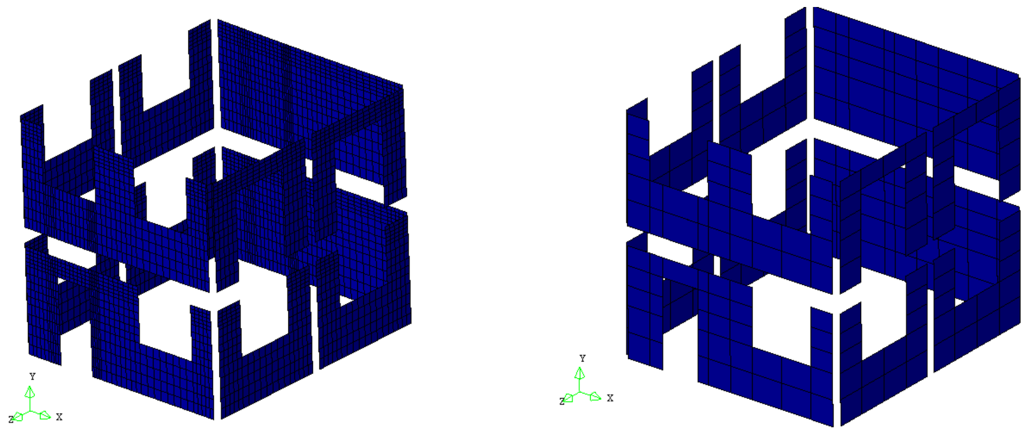

(a) Fine mesh (b) Coarse mesh

Fig. 6 Fine and coarse mesh view

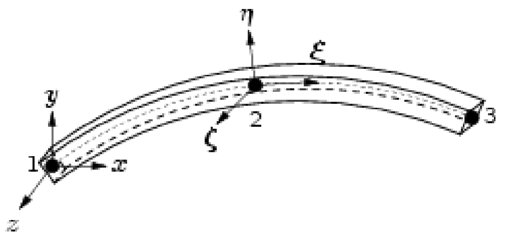

(a) CL18B 3 nodes curved beam element

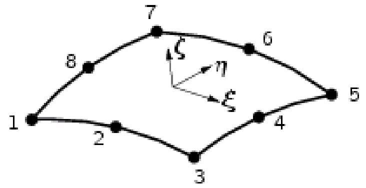

(b) CQ40S eight nodes curved shell element

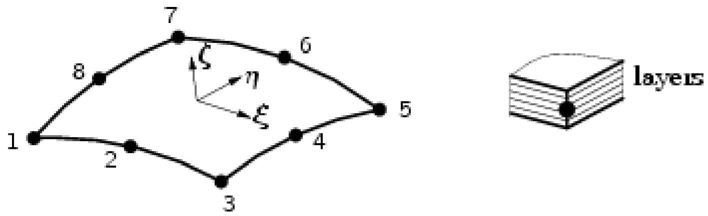

(c) CQ40L eight nodes curved layered shell element for infill wall

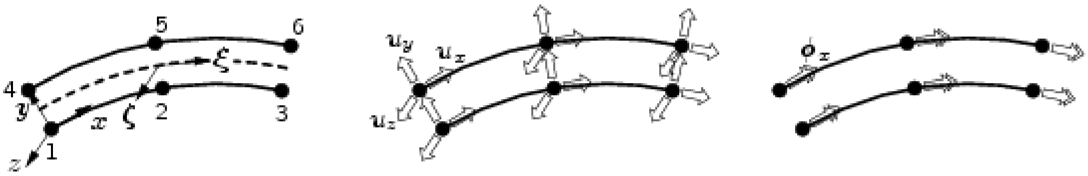

(a) topology (b) displacements

(d) CL24I three nodes interface element for interface media between frame and infill wall

Fig. 7 Element types and topology of numeric models

the CL18B. A CQ40S shell element was used for the slab. This shell element is an 8-node quadrilateral curved shell. For the infill wall, a CQ40L layered shell element was used. This layered shell element is also composed of an 8-node quadrilateral. An interface element was also

Table 4 Maximum values belongs to TLCW and URM models

		TLCW Fine Mesh	TLCW Coarse Mesh	Match Ratio Fine & Coarse (%)	URM Fine Mesh	URM Coarse Mesh	Match Ratio Fine & Coarse (%)
Max. Force Ratio (g)	Trans (+)	0.64	0.68	95	0.37	0.45	82
Displacement (mm)	Trans (+)	5.55	5.15	92	1.67	3.64	46
Max. Force Ratio (g)	Trans (-)	0.62	0.64	97	0.42	0.45	93
Displacement (mm)	Trans (-)	6.62	7.1	93	3.10	2.94	95
Max. Force Ratio (g)	Long (+)	0.47	0.55	85	0.31	0.33	94
Displacement (mm)	Long (+)	9.2	5.52	67	2.47	2.32	94
Max. Force Ratio (g)	Long (-)	0.46	0.54	85	0.34	0.33	97
Displacement (mm)	Long (-)	7.3	5.62	77	3.56	2.19	62

used between the reinforced concrete frame and infill wall. The type of interface element is CL24I. This element is a 3-node line to the shell interface element. The topology of all the elements used can be seen in Fig. 7 (a), (b), (c) and (d) respectively.

The number of elements in the fine mesh is 28562 nodes, while the coarse mesh has only 2821. The purpose of the second analysis is to show how the use of a relatively coarse mesh can affect the results, so that it can be used for dynamic time history analysis. The TLCW reinforced concrete structure was compared with the URM reinforced concrete structure in terms of performance. The URM reinforced concrete structure is composed of a 13 cm scaled (or 20 cm in real scale) uniform thickness infill wall. There are no experimental results for the URM structure, which was modelled with the same boundary and plan geometry condition as the TLCW. The 20 cm uniform thickness infill wall is commonly used in the majority of countries, including Turkey, and its performance level needs to be evaluated. The peak values of the different models in terms of base shear and corresponding displacements can be seen in Table 4.

The absolute maximum experimental base shear ratio of the TLCW model is 0.67 g in the transversal direction, while the numerical simulation provides 0.64 g. For the longitudinal direction the experimental and numerical capacities are 0.47 g and 0.55 g respectively. Comparison of the performance levels can be seen in Fig. 8 and Fig. 9 respectively. In the transversal direction stage 4 was plotted as lines to limit the upper and lower boundaries because the structure was collapsed at the beginning of stage 4. So, there is no displacement record for the longitudinal direction at stage 4 due to damaged instruments. It is estimated that the upper and lower limits of stage 4 are 0.47 g and 0.46 g respectively on the positive and negative sides of longitudinal direction according to the numerical results. The reason for this estimation is the best match between the experimental and numerical results along the transversal direction.

For the URM model, the numerical model reached an average 0.39 g in the transversal direction and 0.32 g in the longitudinal direction with the fine mesh model. However, with the

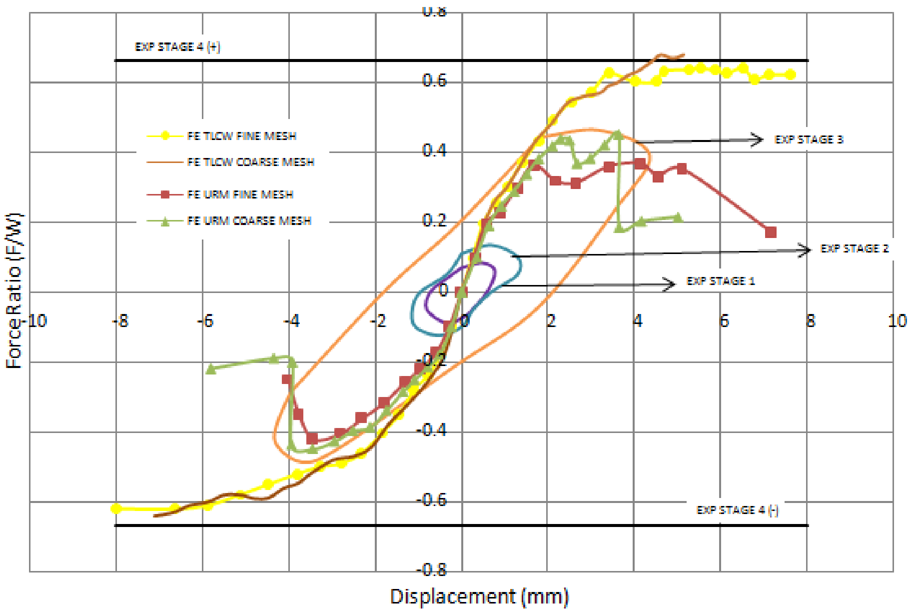

Fig. 8 Force ratio-displacement curves along transversal direction

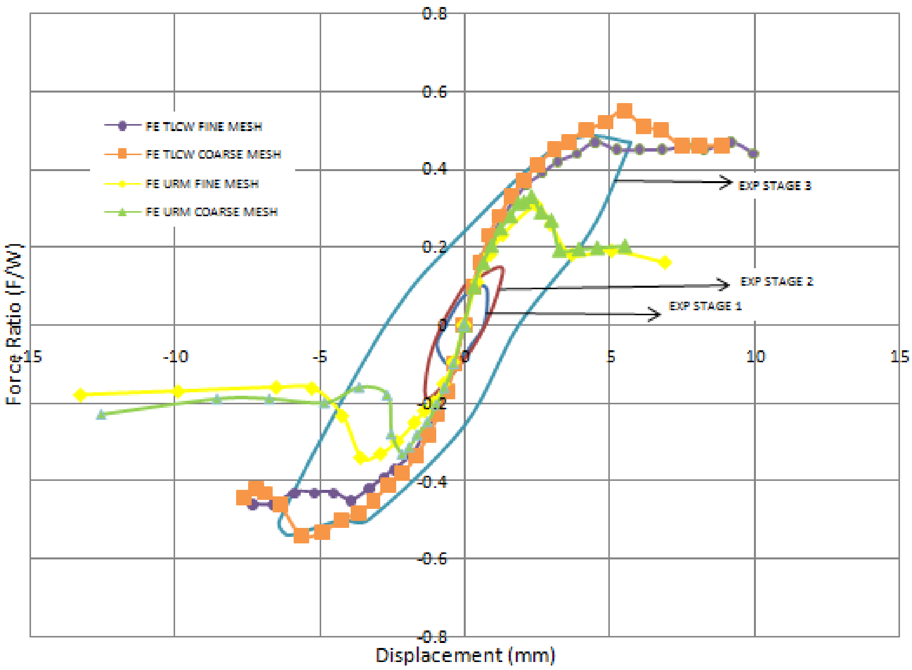

Fig. 9 Force ratio-displacement curves along longitudinal direction

coarse mesh this model reached 0.45 g in the transversal direction and 0.33 g in the longitudinal direction. The comparison of the two pushover curves demonstrates that the maximum error for the TLCW model in terms of the capacity curve for the coarse and fine mesh is only 5.5% in the

Table 5 Performance levels for primary elements of reinforced concrete frames with masonry infill walls

Item	CP	LS	IO
Primary	Extensive cracking and crushing; portions of face course shed.	Extensive cracking and some crushing but wall remains in place. No falling units. Extensive crushing and spalling of veneers at corners of openings.	Minor cracking of masonry infills and veneers. Minor spalling in veneers at a few corner openings.
Secondary	Extensive cracking and crushing; some walls dislodge	Same as primary	Same as primary
Drift	0,6 % transient or permanent	0,5 % transient, % 0,3 permanent	0,1 % transient, negligible permanent

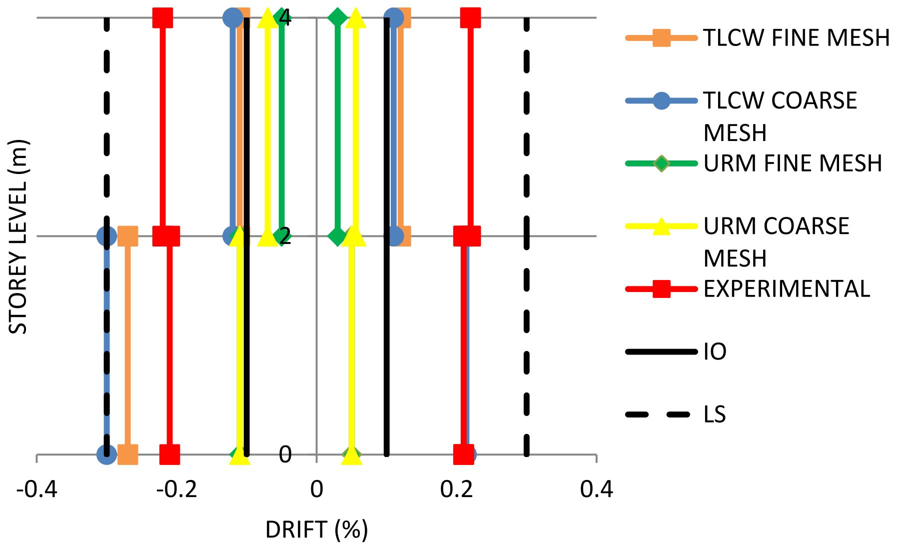

Fig. 10 Storey Level-% Drift curve for fine and coarse meshed models in transversal direction

transversal direction and 15% in the longitudinal direction. On the other hand, for the URM model the maximum error in terms of the capacity curve for the coarse and fine mesh is 13% in the transversal direction and 3% in the longitudinal direction, as seen in Table 4. Still, as the fine mesh is considered more suitable, only this will be considered in the rest of the paper. These results are compared also with the performance levels of the structures given in Table 5 on the basis of ASCE/SEI 41-06.

In the transversal direction, the first storey of the TLCW with fine mesh nearly reached the 0.3% drift capacity in the negative direction, whereas this storey showed more conservative behaviour along the positive direction so this floor remained about the LS line. The experimental results proved that the behaviour of this model is ductile at both storeys, because during the test the structure moved more than desired on the shake table due to the flexible boundary condition. The performance of the tested structure is located between IO and LS. The TLCW fine mesh model showed an extremely good match between the experimental results in the positive and negative directions along the transversal direction at the first storey. However, in finite element

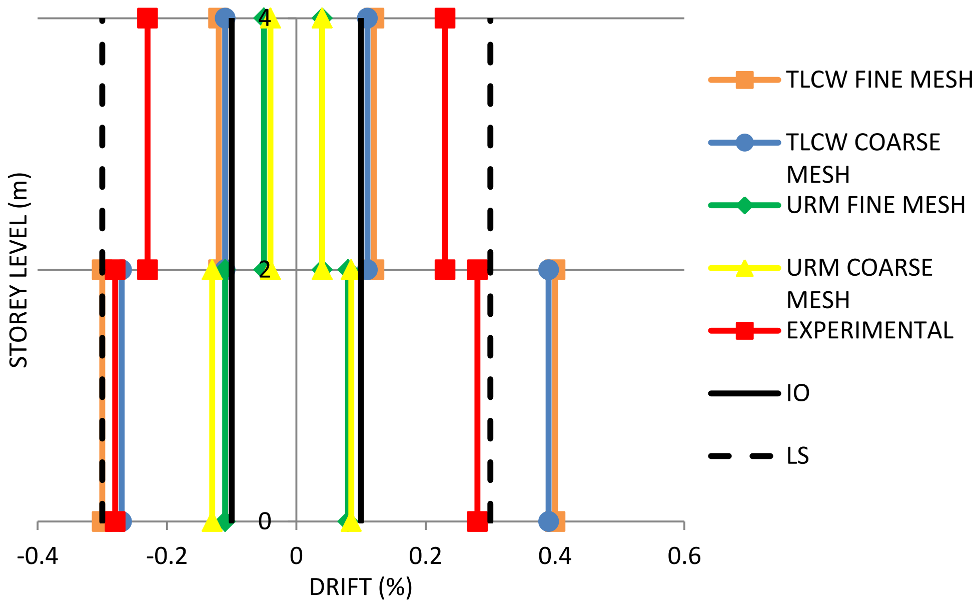

Fig. 11 Storey Level-% Drift curve for fine and coarse meshed models in longitudinal direction

space, nonlinear analysis performed under the perfect boundary condition, for this reason the drift of the second storey showed differences between the experimental results. The rest of the results for the other model for fine and coarse mesh can be seen in Fig. 10.

In the longitudinal direction, the first storey performance of the TLCW model showed a good match between the experimental and numerical drift along the negative direction. For the positive direction, the numerical model showed more ductile behaviour and passed beyond the LS line and experimental drift. However, the first storey performance of the numerical TLCW model is very close to the experimental drift along the negative direction. This performance is located between IO and LS for both models. The second storey performance is near to the IO level. The differences between the experimental and numerical drift at the second storey proved that the structure failed due to the soft storey of the first floor. The performance of the fine and coarse mesh of the URM model can be seen in Fig. 11.

The experimental crack propagation and triggered failure mechanism can be seen in Fig. 12. After nonlinear analysis of the TLCW model, the failure modes and crack propagation can be seen in Fig. 13. As seen, the crack patterns (shown using the maximum principal strains) are compatible with the experimental results. On the basis of the cracks and experimental data, the TLCW structure showed a relatively ductile failure mechanism in the transversal direction. Major cracks propagated at the first floor bottom part of the window through the east and west directions. At the southern part of the structure, diagonal cracks also decreased the bearing capacity of the structure at the first floor, as seen from the positive transversal loading. The weak area is between the window and the door at the first floor at the northern part of the structure. The URM structure has a very close failure pattern to the TLCW, although with lower capacity, and it is not shown here.

The structure began to be damaged at the first floor and then cracks were propagated particularly on the diagonal during the experiment. Due to the soft storey of the first floor, the structure moved along the transversal direction. The transversal direction movement also

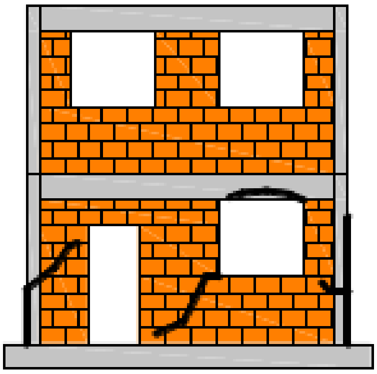

(a) North

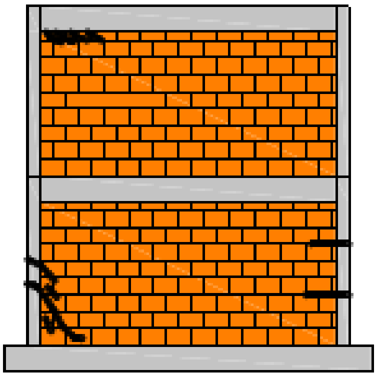

(b) South

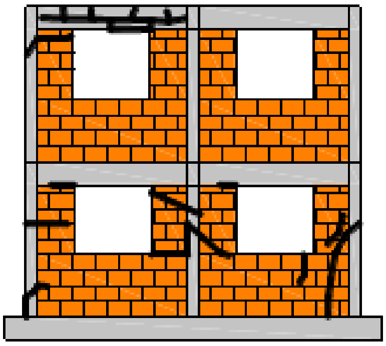

(c) East

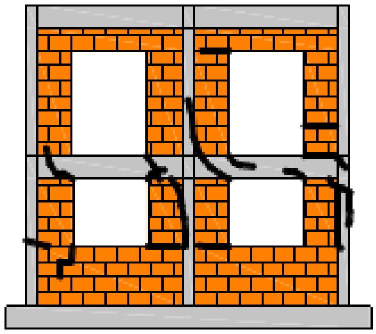

(d) West

Fig. 12 Experimental crack propagation of TLCW at stage 3, before failure (Leite 2014)

corresponded to the movement of the first free vibration period. Then the structure collapsed due to the soft storey beginning of stage 4, which is 1.5 times more than the reference earthquake. The return period of stage 4 is 2475 years. The soft storey movement was triggered by the plastic hinges located on the top of the first floor columns, after which the structure collapsed.

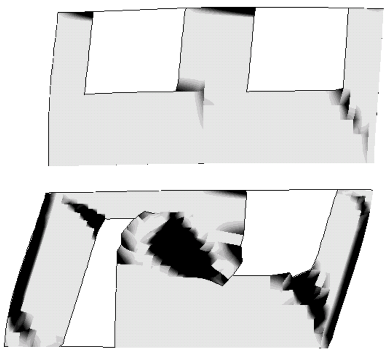

(a) North TLCW numeric model. Loading type: Positive Transversal

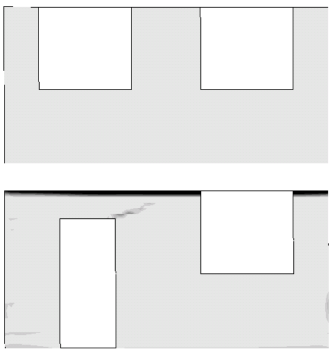

(b) North TLCW numeric model. Loading type: Positive Longitudinal

Fig. 13 Crack pattern of finite element TLCW model in transversal and longitudinal loading

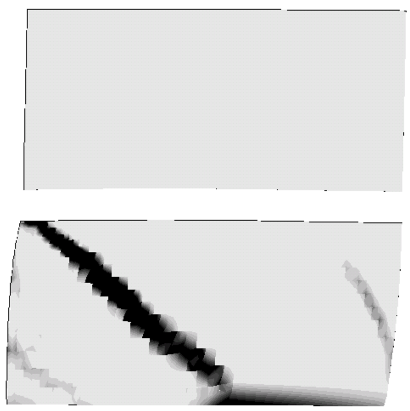

(c) South TLCW numeric model. Loading type: Positive Transversal

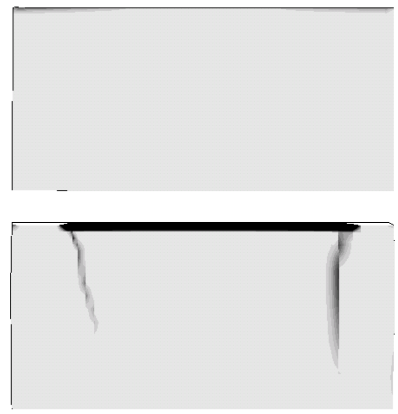

(d) South TLCW numeric model. Loading type: Positive Longitudinal

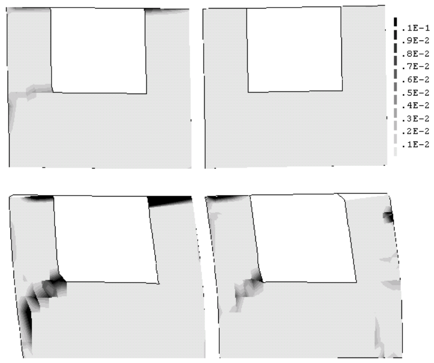

(e) East TLCW numeric model. Loading type: Positive Transversal

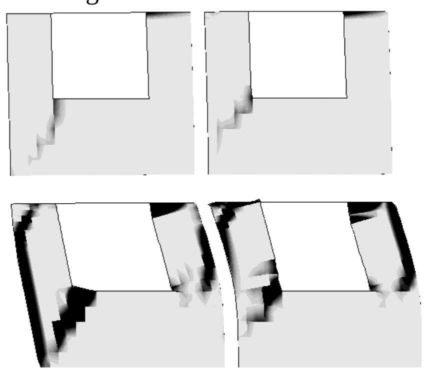

(f) East TLCW numeric model. Loading type: Positive Longitudinal

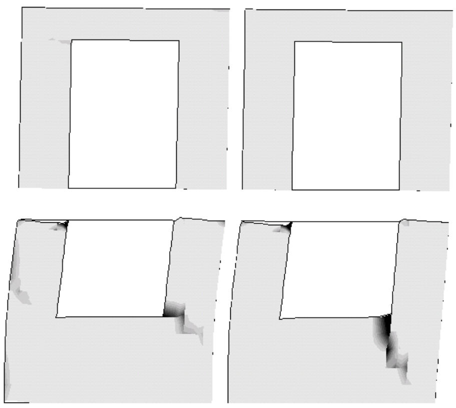

(g) West TLCW numeric model. Loading type: Positive Transversal

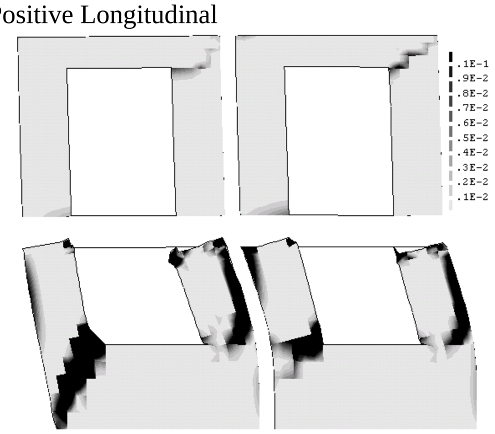

(h) North TLCW numeric model. Loading type: Positive Longitudinal

Fig. 13 Continued

The failure mechanism and collapse of the structure can be seen in Fig. 14 step by step. Fig. 14 also proves that the second storey did not experience significant damage until collapse.

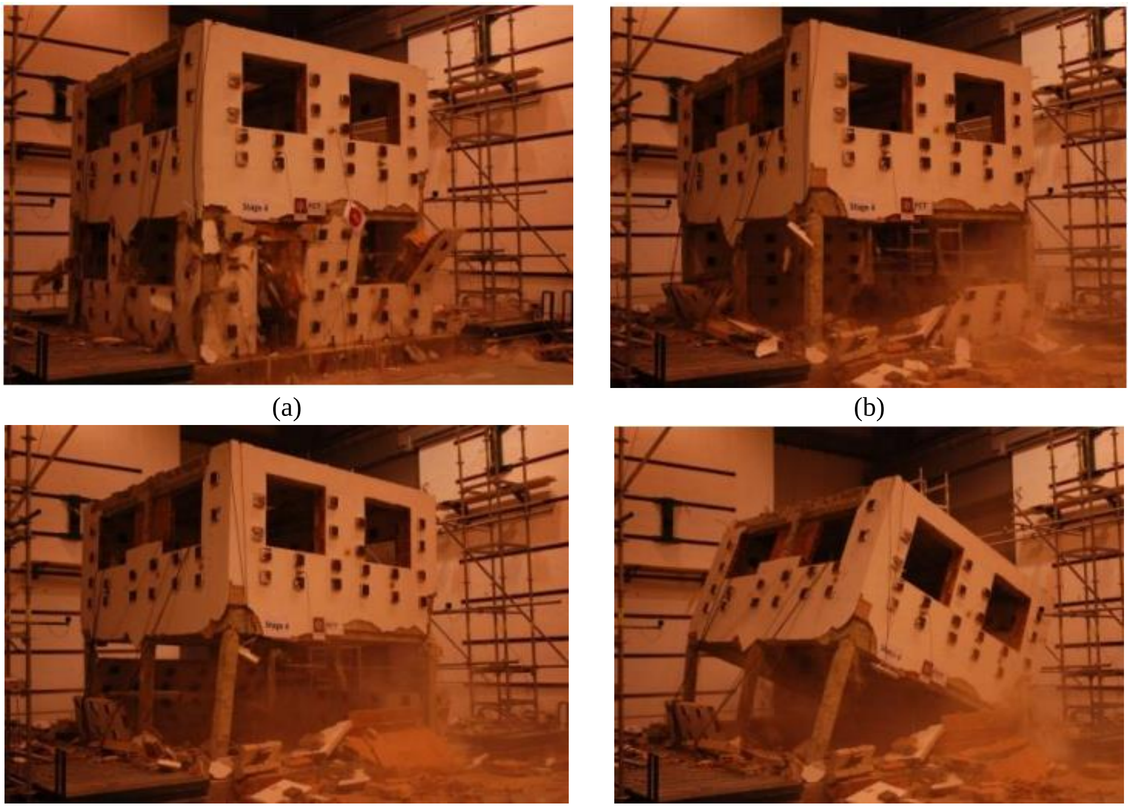

(a) (b) (c) (d)

Fig. 14 Failure mechanism of experimental TLCW model on shake table (Leite 2014)

6. Conclusions

This paper presents the nonlinear static analysis of two case studies of reinforced concrete frames with masonry infill. One of them has a two-leaf cavity wall (TLCW) and the other has a single-leaf wall (URM). Both models have been analysed with a coarse mesh FE model and a fine mesh FE model. There is a 6% difference between the experimental and numerical lateral capacity of the TLCW model in the transversal direction and a 2% difference in the longitudinal direction. Then differences were found of about 10% between the two FE models in terms of the force ratio and 17% in terms of displacement, even though the coarse mesh uses about 1/10 of the degrees of freedom. It is also noted that the TLCW model showed a higher base shear ratio capacity than the URM model in terms of resisting lateral loads, namely 0.64 g in the transversal and 0.5 g in the longitudinal direction, but it also showed a more ductile behaviour. After a certain displacement of the URM model, the infill wall collapsed and only the reinforced concrete frame continued to resist the lateral load. The differences between the two models in terms of base shear are about 35%. The TLCW reinforced concrete frames, which in the presence of excessively strong infill are known as the two-leaf model, proved that this type of infill solution can resist more lateral loads than the conventional type of infill, which is an unreinforced single-leaf wall. 5 cm infill wall thickness differences between the models result in an average 35% base shear and average 42%

displacement at the time of the maximum force ratio. There is only 4% difference between the experimental and fine meshed numerical values in the transversal direction and 2% difference in the longitudinal direction in terms of force ratio (g). The fine meshed model is more conservative due to the early failure of fine mesh elements. The experimental force ratio showed a very good match with the fine meshed TLCW model. Moreover, experimental crack propagation was well simulated by the fine meshed TLCW model. As a result, TLCW infill wall solution is a better structural application for earthquake prone territories than URM infill wall. However, two-leaf cavity reinforced concrete structure showed brittle behavior. In the design phases it is strongly suggested that, to prevent soft storey collapse, the designer should consider this vital point and include the preventive features of the TLCW model.

References

ASCE SEI 41/06, (2007), *Seismic Rehabilitation of Existing Building: ASCE SEI 41/06*, American Society of Civil Engineers, USA.

Barros, R.C. and Almeida, R. (2005), "Pushover analysis of asymmetric three-dimensional building frames", *J. Civil Eng. Manag.*, **11**(1), 3-12.

Bayraktar, A., Coşkun, N. and Yalçın, A. (2007), "Damages of masonry buildings during the July 2, 2004 Doğubayazıt (Ağrı) earthquake in Turkey", *Eng. Fail. Anal.*, **14**, 147-157.

Bruneau, M. (2002), "Building damage from the Marmara, Turkey earthquake of August 17, 1999", *J. Seismol.*, **6**, 357-377.

CEB-FIP Model Code 2010 (2012), *CEB-FIP Model Code 2010 - Final draft, vol. 1.*, Comité Euro-International du Béton.

Chopra, A.K. and Goel, R.K. (2001), "A modal pushover analysis procedure for estimating seismic demands for buildings", *Earthq. Eng. Struct. Dyn.*, **31**, 561-582.

Doğangün, A. (2004), "Performance of reinforced concrete buildings during the May 1, 2003 Bingöl earthquake in Turkey", *Eng. Struct.*, **26,** 841-856.

Dolsek, M. and Fajfar, P. (2005), "Simplified non-linear seismic analysis of infilled reinforced concrete frames", *Earthq. Eng. Struct. Dyn.*, **34**, 49-66.

Eurocode 2 (2004), *Eurocode 2: Design of concrete structures - Part 1-1: General rules and rules for buildings, EN 1992-1-1*, Brussel.

Fajfar, P. (1999), "Capacity spectrum method based on inelastic demand spectra", *Earthq. Eng. Struct. Dyn.*, **28**, 979-993.

Ghobarah, A. (2001), "Performance-based design in earthquake engineering: state of development", *Eng. Struct.*, **23**, 878-884.

Kızılkanat, A., Coşar, A., Koçak, A., Güney, D., Selçuk, M.E. and Yıldırım, M. (2011), *23 October 2011 Van Earthquake Technical Investigation Report*, Yıldız Technical University Press.

Kilar, V. and Fajfar, P. (1997), "Simple push-over analysis of asymmetric buildings", *Earthq. Eng. Struct. Dyn.*, **26**, 233-249.

Krawinkler, H. and Seneviranta, G.D.P.K. (1998), "Pros and cons of a pushover analysis of seismic performance evaluation", *Eng. Struct.*, **20**, 452-464.

Leite, J. (2014), "Design of masonry walls for building enclosures subjected to extreme actions", PhD Dissertation, Minho University, Portugal.

Lourenço, P.B. and Rots, J.G. (1997), "A multi-surface interface model for the analysis of masonry structures", *J. Struct. Eng.*, ASCE, **123**(7), 660-668.

Lourenço, P.B. (2009), "Recent advances in masonry structures: Micromodelling and homogenization, in multiscale modeling in solid mechanics: Computational approaches", Eds. U. Galvanetto, M.H. Ferri Aliabadi, Imperial College Press, 251-294.

Lourenço, P.B., Rots, J.G. and Blaauwendraad, J. (1998), "Continuum model for masonry: parameter estimation and validation", *J. Struct. Eng.*, ASCE, **124**(6), 642-652.

Lourenço P B, (1996), "Computational strategies for masonry structures", PhD Thesis, Delft, Netherland.

Ministry of Construction (2007), Turkey Earthquake Disaster Prevention 2007, Ankara.

Moghadam, A.S. and Tso, W. (2000), "Pushover analysis for asymmetric and set-back multi-story buildings", *12th WCEE*, 1093-1101.

Pereira, M.F.P. (2013), "Avaliação do desempenho das envolventes dos edifícios face à acção dos sismos", PhD Dissertation, University of Minho, Portugal.

Reinhorn, A.M. (1997), "Inelastic analysis techniques in seismic evaluations", *Proceedings of International Workshop on Seismic Design Methodologies for the Next Generation of Codes*, Slovenia.

Salonikios, T., Karakostas, C., Lekidis, V. and Anthoine, A. (2003), "Comparative inelastic pushover analysis of masonry frames", *Eng. Struct.*, **25**, 1515-1523.

Sayın, E., Yön, B., Calayır, Y. and Karaton, M. (2013), "Failures of masonry and adobe buildings during the June 23, 2011 Maden-(Elazığ) earthquake in Turkey", *Eng. Fail. Anal.*, **34**2007 779-791.

Sayın, E., Yön, B., Calayır, Y. and Gör, M., (2014), "Construction failures of masonry and adobe buildings during the 2011 Van earthquakes in Turkey", *Struct. Eng. Mech.*, **51**(3), 503-518.

Selby, R.G. and Vecchio, F.J. (1993), "Three-dimensional constitutive relations for reinforced concrete", Technical Report 93-02, University of Toronto, Department of Civil Engineering, Toronto, Canada.

Structural masonry (1997), An experimental/numerical basis for practical design rules, CUR Report 171, CRC Press, January. (in Dutch)

Tapan, M., Cömert, M., Demir, C., Sayan, Y., Orakcal, K. and İlki, A. (2013), "Failures of structures during the October 23, 2011 Tabanlı (Van) and November 9, 2011 Edremit (Van) earthquakes in Turkey", *Eng. Fail. Anal.*, **34**, 606-628.

Tso, W.K. and Moghadan, A.S. (1996), "Damage assessment of eccentric multistorey buildings using 3-D pushover analysis", *11th World Conference on Earthquake Engineering*, 997-1005.

TNO (2012), "Displacement method Analyser, User's Manual", Release 9.4.4, Netherlands.

Vecchio, F.J. and Collins, M.P. (1986), "The modified compression field theory for reinforced concrete elements subjected to shear", *ACI J.*, **83**(22), 219-231.

Yön, B., Sayın, E. and Köksal, T. S., (2013), "Seismic response of the buildings during the May 19, 2011 Simav, Turkey earthquake" *Earthq. Struct.*, **5**(3), 343-357.

Yön, B. and Calayır, Y. (2014), "Effects of confinement reinforcement and concrete strength on nonlinear behavior of RC buildings", *Comput. Concrete*, **14**(3), 279-297.

Zijl, V.G.P.A.G. (2000), "Computational modeling of masonry creep and shrinkage", PhD Thesis, Delft University of Technology, Nederland.

CC